IGNITION DELAY MEASURMENTS FOR N-DODECANE/N2/AIR MIXTURES AT HIGH PRESSURES

By

Gary Liskovich

A Thesis Submitted to the Graduate
Faculty of Rensselaer Polytechnic Institute
in Partial Fulfillment of the
Requirements for the Degree of
MASTER OF SCIENCE

Major Subject: MECHANICAL ENGINEERING

Approved by the
Examining Committee:

_____
Matthew Oehlschlaeger, Ph.D
Thesis Advisor

_____
Kurt Anderson, Ph.D, Member

_____
Theodorian Borca-Tasciuc, Ph.D, Member

Rensselaer Polytechnic Institute
Troy, New York

November 2017
(For Graduation December 2017)

TABLE OF CONTENTS

LIST OF TABLES

LIST OF FIGURES

ABSTRACT

Ignition delay time measurements have been made in reflected shock experiments for n-dodecane at conditions relevant to diesel engines and those specifically found in the Engine Combustion Network Spray A experiments. The present shock tube studies were carried out for n-dodecane/air mixtures at equivalence ratios of 1.0 and 2.0 for nominal pressures of 40, 60, and 80 atm and also at 60 atm for stoichiometric n-dodecane/O2/N2 mixtures containing 13% and 15% O2, to emulate reduced-O2 mixtures containing exhaust gas recirculation. The parameter space spans the low-temperature, negative-temperature-coefficient, and high-temperature regimes (774 to 1163 K), providing characterization of the complex temperature dependence of ignition important in low-temperature combustion processes and the pressure and oxygen concentration dependencies across the three kinetic regimes. The measurements are compared *a priori* to several recent reduced kinetic models with experiment-modeling deviations near the experimental uncertainties in several cases. To our knowledge, the present experiments represent the first gas-phase homogenous autoignition measurements made for n-dodecane at the extremely high-pressure conditions found in Spray A.

1 INTRODUCTION

Heavy n-alkanes (C_6 and larger) are found in large fractions in all petroleum-based liquid transportation fuels (i.e., gasoline, jet, and diesel fuels), as well as in many synthetic and alternative fuels [1-3]. n-Alkanes are highly reactive [4] relative to branched and cyclo-alkanes, olefins, and aromatics, particularly under low-temperature combustion conditions, and, therefore, in many low-temperature combustion (LTC) engine environments play an important role in governing the overall combustion characteristics of multi-component fuels. n-Dodecane, the subject of the present work, is found in both jet and diesel fuels and has been chosen as an n-alkane representative component in surrogate mixtures designed to emulate both those fuels reported in the literature [5-6].

The development of predictive kinetic models for the autoignition of fuels in at high-pressure engine conditions is critical for the design and optimization of advanced internal combustion engines and the optimization of fuel blends, be they blends of alternative biofuels with petroleum-based fuels or other. Kinetic models must be validated using fundamental experiments at conditions near and overlapping those found in the engines, whose operation and performance they will ultimately be used to predict. However, achieving conditions similar to those found in advanced internal combustion engines (e.g., 50-100 atm near top-dead-center in a compression ignition engine) in controlled reactors or flames is not trivial and often kinetic models are not tested against target data at the conditions for which the models are eventually employed. Shock tube experiments are

---

Portions of this chapter previously appeared in: Kogekar, G., Karakaya, C., Liskovich, G. J., Oehlschlaeger, M. A., DeCaluwe, S. C., & Kee, R. J. (2017). Impact of non-ideal behavior on ignition delay and chemical kinetics in high-pressure shock tube reactors. *Combustion and Flame* (189). doi. 10.1016/201710014

unique in their capability of achieving extreme pressure conditions found in engines and also are configurable so that the autoignition of low-volatility transportation fuels and components can be studied under the high fuel fractions found in engines.

Recent collaborative efforts have been made within the Engine Combustion Network (ECN) [7] to exhaustively characterize canonical spray ignition and combustion experiments at realistic compression-ignition engine conditions and model those experiments using different treatments of turbulence, spray physics, and chemical kinetics as a means to develop computational fluid dynamics (CFD) simulations for spray combustion. One canonical condition of recent experimental study, that has become a benchmark target for CFD simulations, is the Sandia Spray A [7], which has a baseline condition that is n-dodecane injection into an ambient gas at temperature of 900 K, density of 22.8 kg/m3 (~60 atm), and containing 15% O2. Perturbations in temperature, density/pressure, O2 concentration, injection parameters, and fuel have been widely studied experimental within the ECN in both the Spray A and other configurations [8-11] and modeled using different CFD approaches [12-17]. However, to date ignition delay and other kinetic studies to validate the kinetic models used in those spray combustion simulations are lacking and kinetic models are presently employed under mostly extrapolative conditions in spray CFD simulations.

Prior ignition delay studies for n-dodecane [18-21] have been carried out in shock tubes under the conditions given in Table 1.1 with few studies approaching the conditions found in the n-dodecane Spray A experiment (60 atm, fuel-rich, reduced O2 concentrations). Autoignition experiments have been also been reported for n-decane in both shock tubes [20,22-23] and rapid compression machines [24], with two notable shock

tube studies reporting ignition delay at the high-pressure conditions considered in the ECN studies. Pfahl et al. [22] measured ignition delay times for φ = 0.5-2 n-decane/air mixtures at 13-50 atm and 700-1300 K, these measurements have been used as targets for reduced kinetic models within the ECN, and Zhukov et al. [23] has reported ignition delay for φ = 0.5-1.0 n-decane/air mixtures at 10-80 atm and 800-1300 K. Additionally, single-pulse shock tube speciation studies of n-dodecane oxidation and pyrolysis at realistic engine conditions (19-74 atm, 867-1739 K) have been reported by Malewicki and Brezinsky [25]. Prior work on the kinetic modeling of n-dodecane has resulted in several detailed kinetic mechanisms (e.g., [4,25-31]) for the description of its oxidation under low- and high-temperature conditions. Within the ECN and similarly focused research efforts, several of these mechanisms have been reduced for implementation into CFD [12-13,32-34].

Table 1.1 Conditions of prior shock tube and RCM measurements for n-dodecane ignition delay.

Authors	**T [K]**	**P [atm]**	**Φ and mixture**
Davidson et al. [18]	1050−1350	5.8−6.7	0.5, fuel/21% O_2/Ar
Vasu et al. [19]	727−1422	15−34	0.5, 1.0, fuel/air
Shen et al. [20]	875−1250	14, 40	0.5, 1.0, fuel/air
Haylett et al. [21]	850−1350	4−9	0.1-2.0, fuel/21% O_2/Ar
Present study	775−1160	40, 60, 80	1.0, 2.0, see Table 2.1

Here shock tube ignition delay times are reported for n-dodecane at the conditions encompassing those found in the Sandia Spray A experiment. The present condition space has been chosen to cover a parametric variation of pressure, temperature, and oxygen concentration considered within the spray experiments and provides data at fuel-rich conditions where local ignition within typical spray environments occurs. The data provides evaluation of available reduced n-dodecane kinetic models and in the future will

allow for the validation of new models at realistic compression ignition engine conditions where data is typically not available.

2 EXPERIMENTAL METHODS

Ignition delay measurements were performed in the Rensselaer heated high-pressure shock tube using the reflected shock technique; see Shen and Oehlschlaeger et al. [35] and Wang et al. [36] for details of the experimental setup and ignition delay measurement technique. In the present experiments n-dodecane at 99+% purity from Sigma Aldrich and O2 and N2 at 99.995% purity from Noble Gas were used. The shock tube, reactant mixing vessel, and gas transfer lines were uniformly heated to temperatures from 160 to 180 ˚C using an electric heating system. Mixtures were made inside the reactant mixing vessel by injecting liquid n-dodecane directly into the vessel, allowing it to fully vaporize, and then adding N2 and O2 in that order, with the mixture fractions determined manometrically. Prior sampling studies [36] have demonstrated the accuracy of gaseous fuel/air mixtures made using this method. Here we estimate the mixture reported fuel fractions are accurate to within ±4%. The reactant mixtures studied are defined in Table 2.1 and include stoichiometric and rich ($\varphi = 2$) conditions, fuel-air mixtures (~20% O2) and dilute mixtures emulative of in-cylinder mixtures containing exhaust gas recirculation (EGR), pressures from 40 to 80 atm, and temperatures that span the low- to high-temperature ignition regimes. These conditions represent a wide range of conditions relevant to diesel and

Portions of this chapter previously appeared in: Kogekar, G., Karakaya, C., Liskovich, G. J., Oehlschlaeger, M. A., DeCaluwe, S. C., & Kee, R. J. (2017). Impact of non-ideal behavior on ignition delay and chemical kinetics in high-pressure shock tube reactors. *Combustion and Flame* (189). doi. 10.1016/201710014

advanced compression ignition internal combustion engines and also future high-pressure-ratio gas turbines. The conditions were specifically chosen as they overlap those considered in Sandia Spray A within the ECN [7].

Table 2.1 Experimental conditions for n-dodecane/O_2/N_2 ignition delay measurements.

n-dodecane [mol-%]	**O_2 [mol-%]**	**N_2 [mol-%]**	**φ**	**P [atm]**	**T [K]**
1.12	20.77	78.10	1.0	40, 60, 80	775-1160
2.22	20.54	77.24	2.0	40, 60	800-1120
0.811	15.00	84.19	1.0	60	840-1110
0.703	13.00	86.30	1.0	60	840-1140

For the present high-pressure conditions considered, where ignition delay times are relatively short, the shock tube was driven with pure helium, providing sufficient reflected shock test times of around a millisecond. Ignition delay times were determined using a combination of dynamic pressure measurements made with a pressure transducer (Kistler 603B1) located 2 cm from the shock tube end wall and hydroxyl radical chemiluminescence observed through the end wall. An example ignition delay measurement is provided in Fig. 2.1 For temperatures within the low-temperature and the lower temperature portion of the negative-temperature-coefficient (NTC) regime, two-stage ignition was observed (see Fig. 2.1) where the pressure clearly shows first-stage ignition followed by an induction period to a very strong second-stage “hot” ignition. Total ignition delay times were determined using the end wall OH chemiluminescence signal by extrapolating the maximum gradient in that signal to the baseline to define the onset of ignition. Time-zero was defined as the time of shock reflection at the end wall and was determined by extrapolation of the shock trajectory to the end wall as measured using a series of pressure transducers spaced over the last meter of driven section.

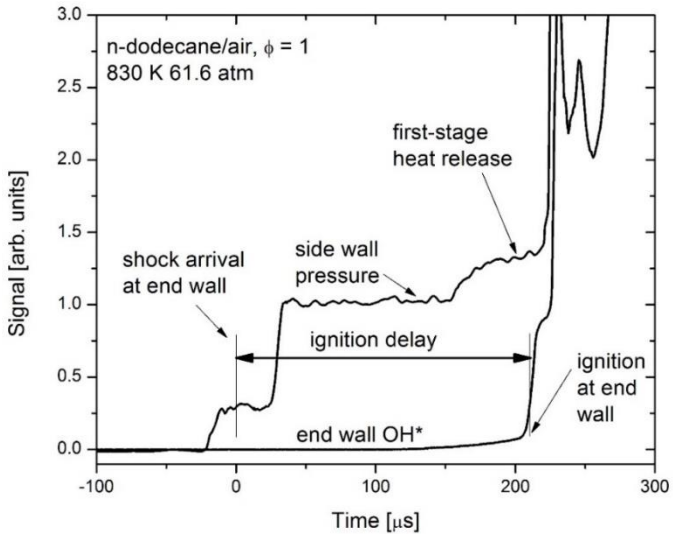

Fig. 2.1 Example pressure and OH chemiluminescence signals for a stoichiometric n-dodecane/air ignition delay measurement.

In the present work, the normalized pressure rise following the reflected shock heating, due to viscous gasdynamics, was in the range of dP/dt = 2-5 %ms-1. However, the ignition delay determinations are negligibly influenced by this pressure rise because ignition delay times are relatively short (< 1 ms) at the high-pressure conditions considered. Hence, this pressure gradient was not considered in the kinetic modeling comparisons presented in the next section. The temperature and pressure behind the reflected shock wave have uncertainties of around ±1.0 to ±1.5% and ±1.5 to ±2.0%, respectively. These condition uncertainties, uncertainties in mixture fractions, and uncertainties in the definition of time zero and the onset of ignition from the signals lead to an estimated integrated uncertainty of ±20% in the reported ignition delay. For a tabulation of all ignition delay measurements see the appended supplementary material.

3 RESULTS AND DISCUSSION

Measured ignition delay times for n-dodecane/air mixtures at 40, 60, and 80 atm and equivalence ratios of 1.0 and 2.0 for a temperature range of 775 to 1160 K are shown in Fig. 3.1. For these conditions the ignition delay times span durations of approximately 60 to 400 μs and illustrate negative-temperature-coefficient (NTC) behavior with a transition from low-temperature (positive overall activation energy) to NTC (overall activation energy of zero to slightly negative) behavior around 850 K and a transition from NTC to high-temperature (positive overall activation energy) behavior around 1000 K. The ignition delay times decrease with increasing pressure across the entire temperature domain but with stronger pressure dependence in the NTC than at high temperatures. Ignition delay times for $\varphi = 2$ mixtures are approximately 50% shorter than for $\varphi = 1$. Measured ignition delay times for reduced O2 concentration mixtures are shown in Fig. 3.2 with similar NTC behavior apparent and increased ignition delay times with decreasing O2 concentration. Again, the dependence on O2 concentration is stronger in for NTC temperatures than at high temperatures.

Portions of this chapter previously appeared in: Kogekar, G., Karakaya, C., Liskovich, G. J., Oehlschlaeger, M. A., DeCaluwe, S. C., & Kee, R. J. (2017). Impact of non-ideal behavior on ignition delay and chemical kinetics in high-pressure shock tube reactors. *Combustion and Flame* (189). doi. 10.1016/201710014

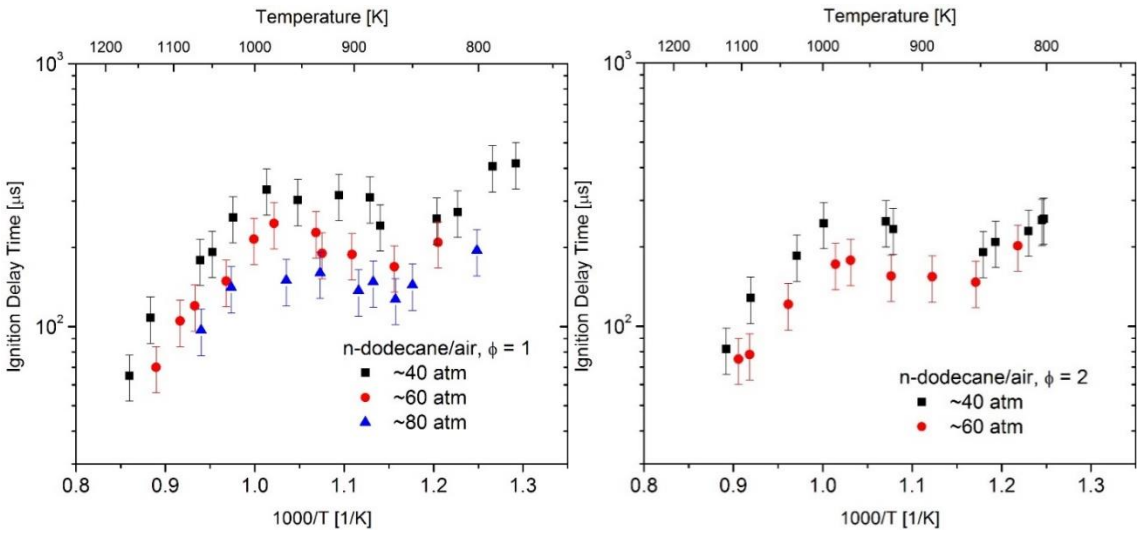

Fig. 3.1 Ignition delay measurements for n-dodecane/air mixtures at equivalence ratios of 1.0 (left) and 2.0 (right) and pressures around 40, 60, and 80 atm.

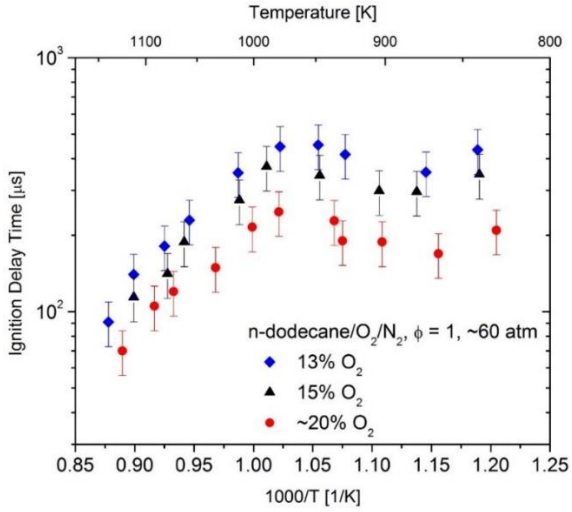

Fig. 3.2 Ignition delay measurements for stoichiometric n-dodecane/O2/N2 mixtures a pressure around 60 atm.

While there are no data available within the literature to directly compare the present experimental results, the data are compared in Fig. 3.3 to shock tube ignition delay measurements carried out for n-dodecane at lower pressure (20 atm) by Vasu et al. and with results for n-decane reported at 50 atm by Pfahl et al. [22] and 80 atm by Zhukov et al. [23]. The literature results all exhibit similar temperature dependence to the present

results and at high pressures the n-decane and n-dodecane results are in quantitative agreement within the experimental scatter/uncertainty as expected based on the similarity of ignition delay times for large n-alkanes for strong mixtures (i.e., containing high fuel fractions) [4,20]. Further comparisons of the present study with the 20 atm n-dodecane measurements of Vasu et al. [19], made in the following section in Fig. 3.7, illustrate that the two data sets are in very good agreement when compared by extrapolating the present ignition delay data and observed pressure dependence to lower pressure.

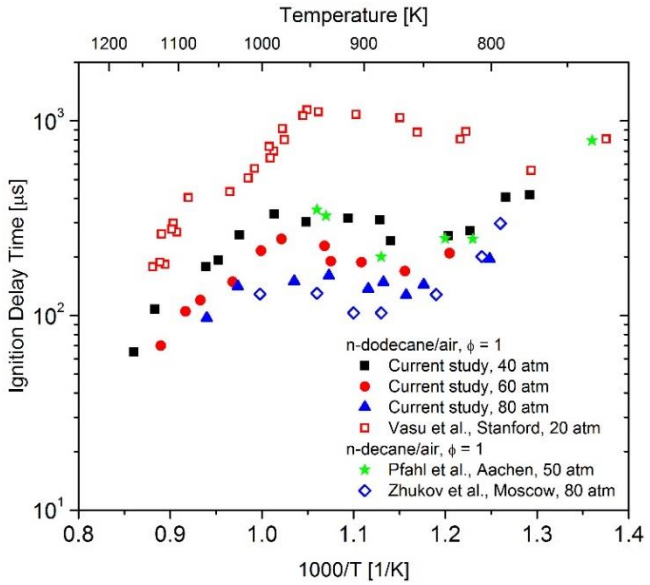

Fig. 3.3 Comparison of present ignition delay measurements for stoichiometric n-dodecane/air to previous measurements for n-dodecane [19] and n-decane [22-23] from the literature.

Many detailed and reduced kinetic models exist in the literature for the description of n-alkane oxidation and ignition. Here comparisons are made to four recently published reduced n-dodecane kinetic models [12,31-33]. These four models all are reductions, extensions, or modifications of the detailed kinetic models produced by the group at Lawrence Livermore National Laboratory (LLNL) [4,28] and have been chosen because

they have been considered within the Engine Combustion Network (ECN) [7] for modeling Sandia Spray A (n-dodecane high-pressure spray ignition experiment) using CFD approaches. A brief description of the four models is provided in Table 3.1. The details regarding the source of the reactions and rate coefficients and reduction and optimization methods are left to the references describing these models but effectively the Luo et al. model is a reduction of LLNL chemistry with no modifications and the other three are reductions of LLNL chemistry with modifications to reflect improvements or differences within the kinetic modeling literature for rate parameters and/or optimization of rate parameters to best fit ignition delay data from the literature.

Table 3.1 Reduced kinetic models compared to measurements in Figs. 3.4-3.8.

Authors	**No. species / reactions**	**Description**
Luo et al. [12]	105 / 420	Reduced from detailed LLNL mechanism [28] with no modifications or adjustments to rate parameters; reproduces the ignition delay predictions of the LLNL mechanism at the conditions of the present study.
Narayanaswamy et al. [32]	255 / 2289	Reduced from detailed LLNL mechanism [28] with modifications to the low- and high-temperature chemistry: H_2/O_2, ketohydroperoxide formation, H-abstraction from n-dodecane, H-abstraction from and decomposition of alkenes, decomposition of alkenyl radicals.
Wang et al. [33]	100 / 432	Reduced from detailed LLNL mechanism [4], with significant adjustments to fit literature n-alkane ignition delay times [37].
Cai et al. [31]	624 / 2727	Starting with original LLNL reaction pathways, rate coefficients are optimized through a Bayesian approach [38-39] to best fit an n-alkane ignition delay database.

Comparisons of measurements with the predictions of the four kinetic models are provided in Figs. 3.4-3.8. Comparisons on Arrhenius axes in Figs. 3.4 and 3.5 indicate the model fidelity for prediction of ignition delay and its temperature dependence. In all cases, the unoptimized Luo et al. model overpredicts high- and low-temperature ignition delay and overpredicts the transition temperatures but reasonably captures ignition delay in the NTC. The optimized Cai et al. model systematically underpredicts ignition delay for n-

dodecane/air mixtures but performs very well at reduced oxygen concentrations. The Narayanaswamy et al. and Wang et al. models perform remarkably well across the entire parameter space with the Narayanaswamy model slightly diverging from measurement at the very lowest temperatures. A global comparison of the model performance for predicting the measured ignition delay is given in Fig. 3.6 in terms the root-mean-square deviation (RMSD) in experiment and model predictions: $RMSD = \sqrt{\frac{\left[\frac{\tau_{model}-\tau_{exp}}{\tau_{exp}}\right]^2}{n}}$, where τ_{model} is the model-predicted ignition delay, τ_{exp} the measured ignition delay, and n the total number of experiments performed (n = 73). Like the comparisons on Arrhenius axes, Fig. 3.6 shows the Narayanaswamy et al. and Wang et al. models best capture measured ignition delay with performance near the ±20% experimental uncertainty. The Wang et al. model is the most highly adjusted model; while it starts from the base LLNL chemistry, all isomers have been lumped and all reaction rate coefficients along the low-temperature oxidation pathway from the first O2 addition to alkyl radicals to ketone decomposition have been adjusted to best fit previous ignition delay times for n-heptane [40-41], n-decane [20,22-23], and n-dodecane [19].

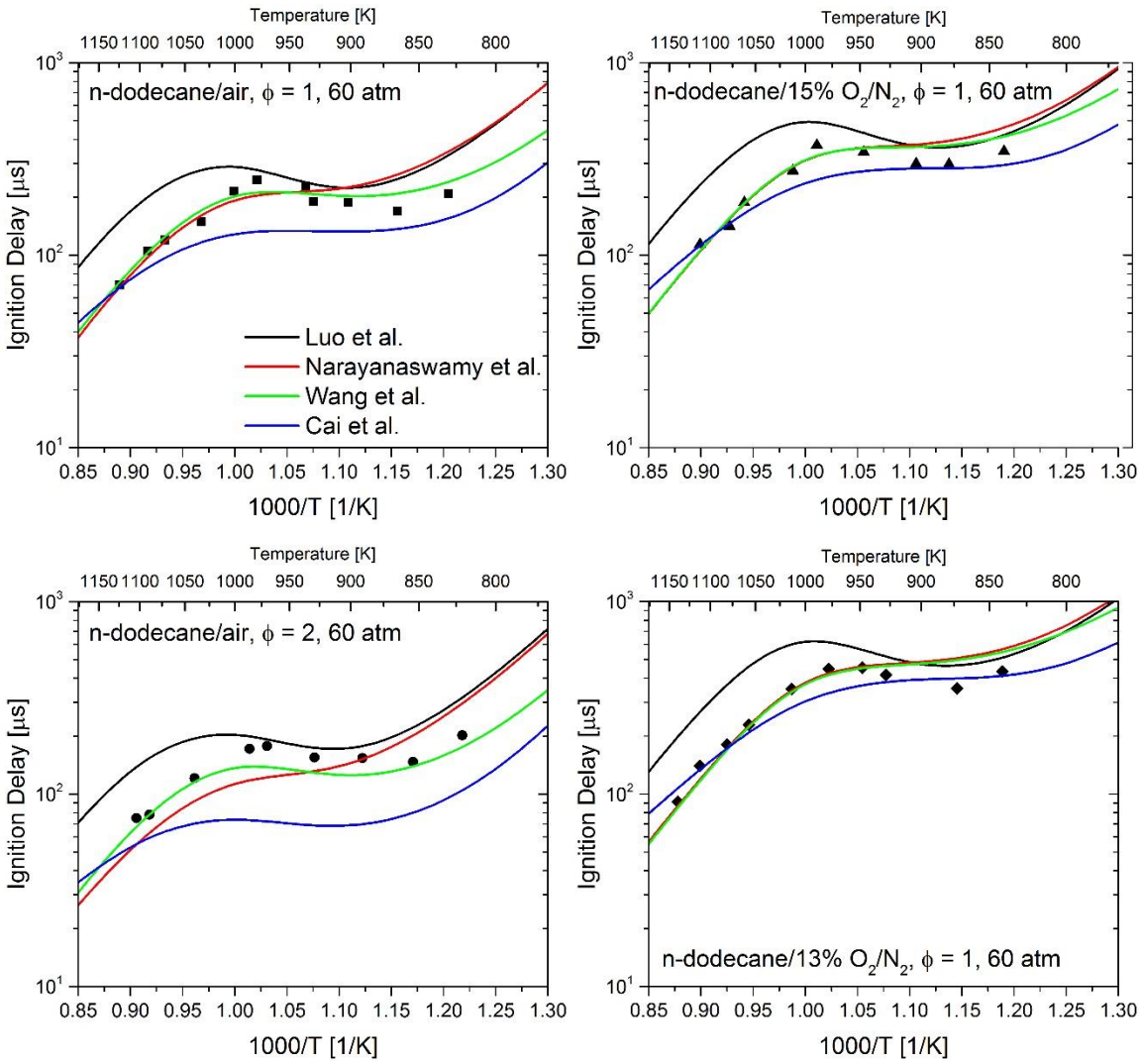

Fig. 3.4 Comparison of 60 atm ignition delay measurements (symbols) with kinetic modeling predictions (lines) [12,31-33].

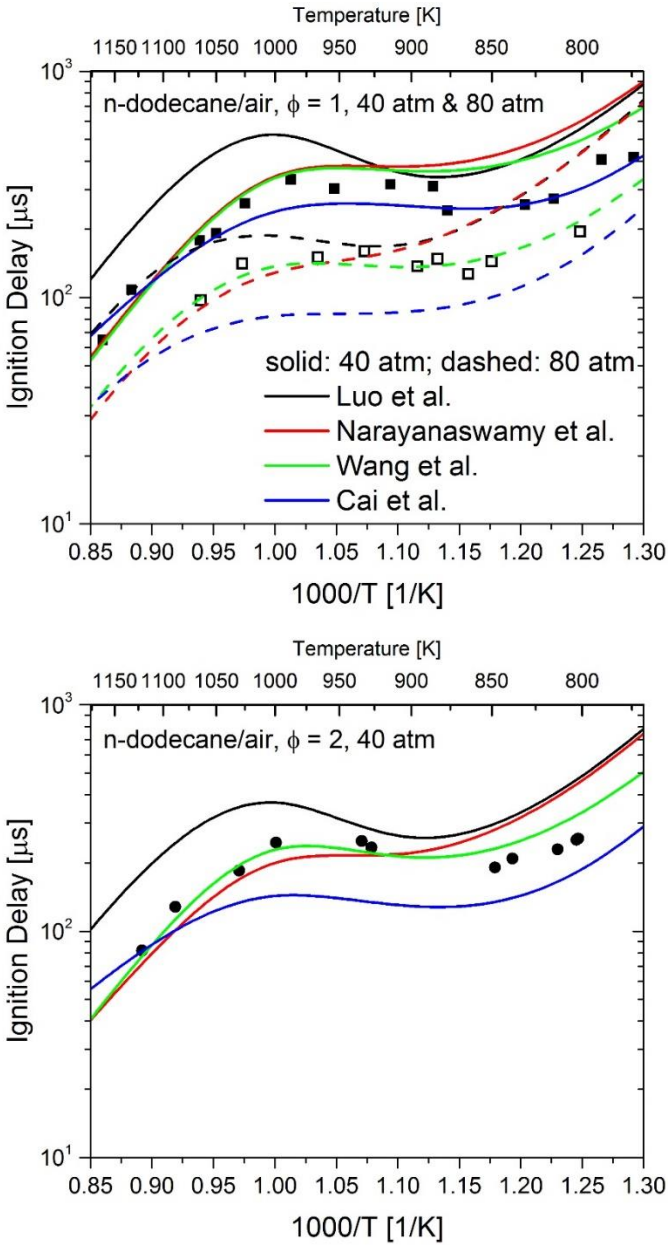

Fig. 3.5 Comparison of 40 atm (closed symbols) and 80 atm (open symbols) ignition delay measurements with kinetic modeling predictions (solid lines: 40 atm; dashed lines: 80 atm) [12,31-33].

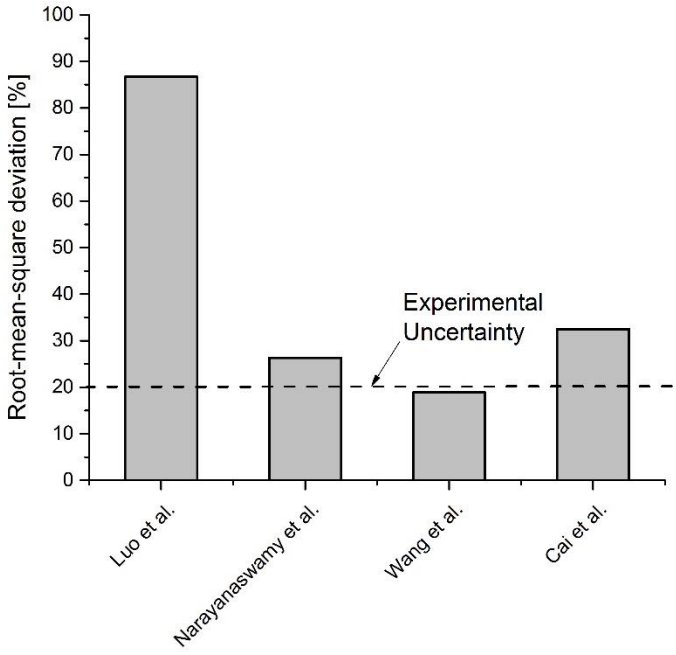

Fig. 3.6 Global performance of the kinetic models tested [12,31-33]: root-mean square deviation in experiment versus model predications for all measurements.

The measured and model-predicted dependence of ignition delay on pressure and oxygen concentration are illustrated in Figs. 3.7 and 3.8. The pressure and oxygen concentration dependencies are quantified at three temperatures where sufficient data exists: 900, 1000, and 1100 K. The pressure dependence in Fig. 3.7 also includes results of the Vasu et al. [19] study at 20 atm which are in agreement with an extrapolation of the present results. Again the models vary in their prediction of ignition delay but all the models capture the measured pressure and O2 concentration dependencies very well (i.e., the experimental slopes in Figs. 3.7 and 3.8 are captured by the models).

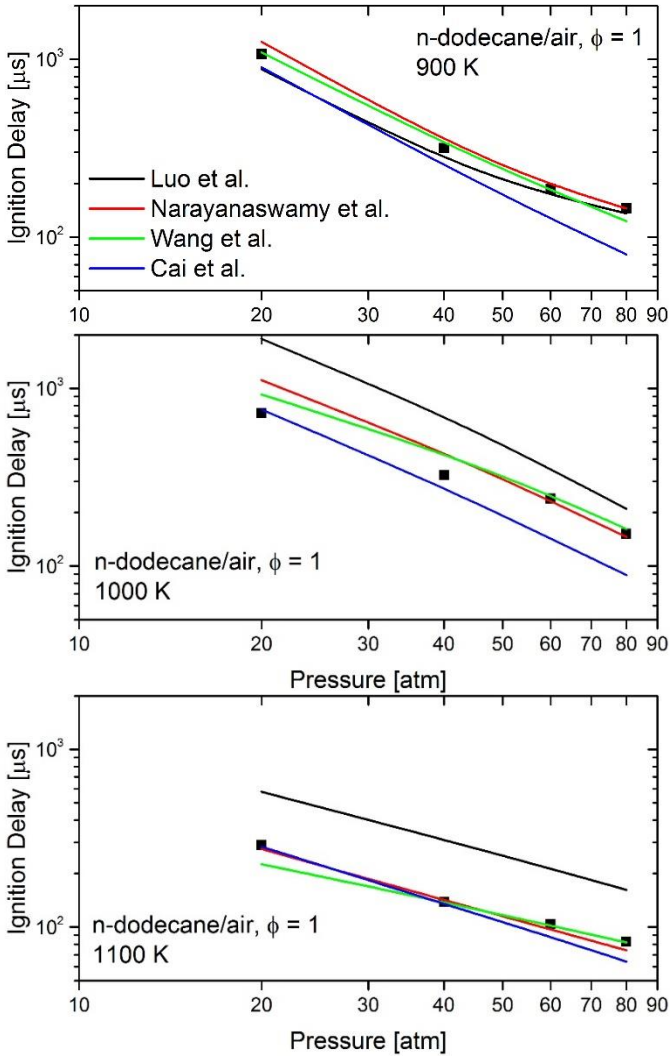

Fig. 3.7 Dependence of measured ignition delay on pressure (at stoichiometric n-dodecane/air conditions) with comparisons to kinetic models [12,31-33]. Data at 20 atm from Vasu et al. [19].

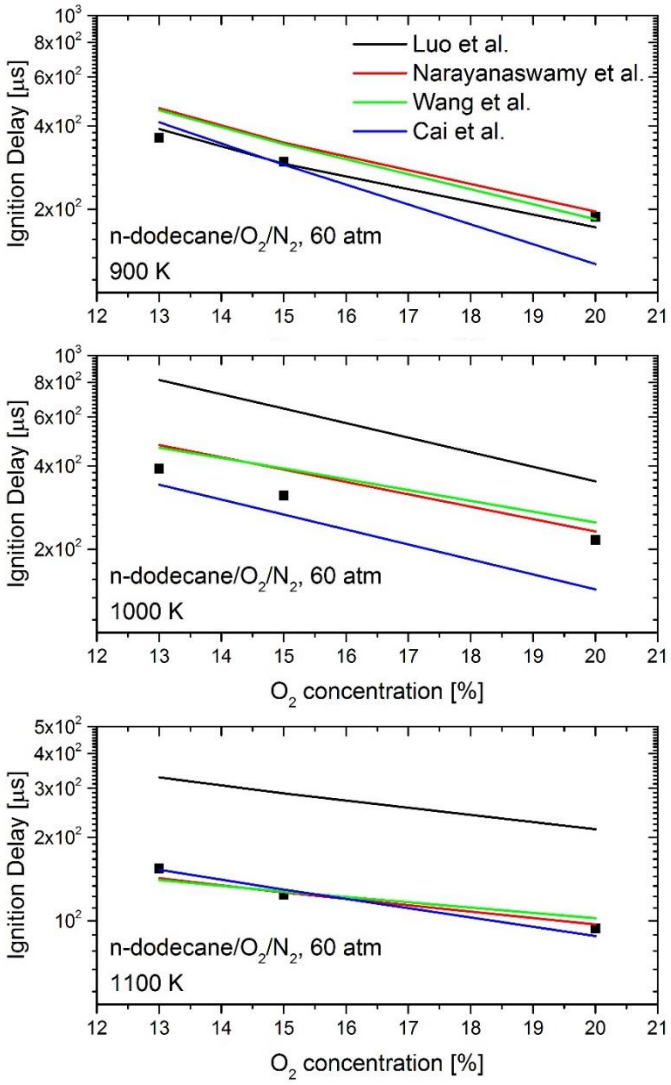

Fig. 3.8 Dependence of measured ignition delay on oxygen concentration (at 60 atm) with comparisons to kinetic models [12,31-33].

Inspection of the four kinetic models [12,31-33] examined in Figs. 3.4-3.8 was carried out using reaction path, rate of production, and sensitivity analyses to determine what model rate parameters and reaction paths lead to the observed differences in ignition delay predictions. Interestingly, despite the fact that all four models start with the base LLNL chemistry, the reductions and optimization undertaken in their development results in

ignition delay predictions that are sensitive to different chemistry as illustrated in the ignition delay sensitivity shown in Fig. 3.9. Important differences exist within the models for the rates of H abstraction reactions from n-dodecane, the primary n-dodecane removal mechanism under the present conditions. The two reactions that remove most of the n-dodecane are H abstraction by OH and HO2. The Luo et al. [12] model predicts nearly 100% of the n-dodecane is removed via H abstraction by OH at the Fig. 3.9 conditions. The other three models, however, have increased rates for H abstraction by HO2 and a larger fraction of n-dodecane removal occurs via this channel: 8% in the Narayanaswamy et al. model [32], 61% in the Wang et al. model [33], and 9% in the Cai et al. model [31] at the Fig. 3.9 conditions. Other important model differences include the removal pathways for the C12H25 radicals that are formed from n-dodecane. In the Luo et al. and Narayanaswamy et al. models, C12H25 primarily undergoes low-temperature oxidation (R + O2 → RO2 → QOOH (+O2) → OOQOOH → OH + ketohydroperoxide → OH + products); hence, in these two cases the ignition delay sensitivity is largely dominated by low-temperature oxidation reactions and H abstraction from n-dodecane. In the Wang et al. model a significant fraction of the C12H25 radical directly fragments to C6H13 and C6H12 products (~90% for the Fig. 3.9 conditions) which then oxidize and further fragment leading to ignition delay sensitivity that is controlled by H abstraction from n-dodecane, oxidation and fragmentation of C6 species, and small molecule oxidation chemistry. In the Cai et al. model the C12H25 radicals primarily undergo low-temperature oxidation; however, in the Cai et al. model the overall rate of low-temperature oxidation has been increased through optimization to fit prior literature ignition delay data, most of which is at lower pressures. This leads to an overall ignition delay that is limited to a greater

extent by small molecule oxidation that occurs after first-stage heat release; i.e., at the present conditions, first-stage heat release is more rapid within the Cai et al. model compared to the other models and leads to the formation of small molecules that undergo a slower second-stage heat release that rate limits ignition. This not only leads to ignition delay sensitivity to small fmolecule chemistry within the Cai et al. model but also an underprediction of ignition delay as shown in Figs. 3.4-3.5. The differences in the four sensitivity analyses shown in Fig. 3.9, indicate a synergism between large and small molecule chemistry that illustrates the importance of both in predicting low-temperature and NTC autoignition. Additionally, the optimizations that have been carried out for some of the models, leading to improved prediction of ignition delay, have significantly changed the chemistry and sensitivities such that these models have perturbed heat release rates or magnitudes of low- versus high-temperature heat release that will affect their prediction of other combustion phenomena (e.g., flame dynamics, cool flame extinction).

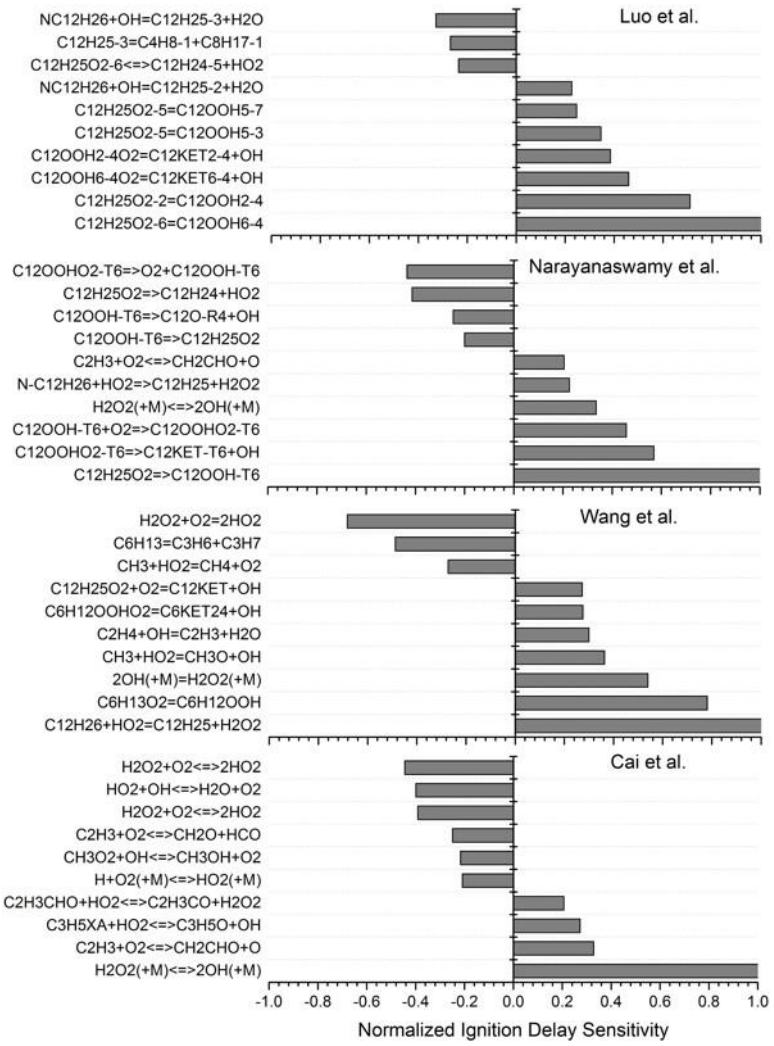

Fig. 3.9 Normalized sensitivity for ignition delay for the four kinetic models investigated [12,31-33]; conditions: stoichiometric n-dodecane/air at 900 K and 60 atm. Sensitivity has been defined as the change in ignition delay for a factor of two change in rate coefficients ($\tau_{2k} - \tau_k$) divided by the baseline ignition delay (τ_k). Those sensitivities are then normalized by the maximum sensitivity for a model, such that sensitivities can be compared across models.

4 CONCULSIONS

Ignition delay time measurements for n-dodecane are reported at high pressures (40, 60, and 80 atm) for n-dodecane/air mixtures at equivalence ratios of 1.0 and 2.0 and for stoichiometric n-dodecane/O2/N2 mixtures containing reduced oxygen concentrations (13 and 15%). Measurements were performed for temperatures (774 to 1163 K) spanning the low-temperature, negative-temperature-coefficient, and high-temperature regimes. To our knowledge, these are the first ignition delay measurements for n-dodecane at high-pressure conditions overlapping those found in the Engine Combustion Network Spray A experiment for high-compression-ratio diesel and advanced compression ignition engines. The experiments are compared to four reduced kinetic models from the recent literature [12,31-33]. All models capture the experimental pressure and oxygen concentration dependencies and two models, those of Narayanaswamy et al. [32] and Wang et al. [33], quantitatively predict ignition delay with root-mean-square deviation of ±20 to ±30%, near the experimental uncertainty limits.

WORKS CITED

[1] Dagaut P, Cathonnet M. "The ignition, oxidation, and combustion of kerosene: A review of experimental and kinetic modeling." *Prog Energy Combust Sci*, vol. 32, no. 5, pp. 48-92, 2006.

[2] Colket M, Edwards T, Williams S, Cernansky NP, Miller DL, Egolfopoulos F, Lindstedt P, Sheshadri K, Dryer FL, Law CK, Friend D, Lenhert DB, Pitsch H, Sarofim A, Smooke M, and Tsang W. "Development of an experimental database and kinetic models for surrogate jet fuels." *45th AIAA ASME,* 2007.

[3] Pitz WJ, Mueller CJ. "Recent progress in the development of diesel surrogate fuels." *Prog Energy Combust Sci*, vol. 37, no. 3, pp. 330-350, June 2011.

[4] Westbrook CK, Pitz WJ, Herbinet O, Curran HJ, Silke EJ. "A comprehensive detailed chemical kinetic reaction mechanism for combustion of n-alkane hydrocarbons from n-octane to n-hexadecane." *Combust Flame,* vol. 156, no. 1, pp. 181-199, Jan 2009.

[5] Violi A, Yan S, Eddings EG, Sarofim AF, Granata S, Faravelli T, Ranzi E. "Experimental formulation and kinetic model for JP-8 surrogate mixtures." *Combust Sci Technol*, vol. 174, no. 11-12, pp. 399-417, Sep 2010.

[6] Dooley S, Won SH, Heyne J, Farouk TI, Ju Y, Dryer FL, Kumar K, Xui X, Sung CJ, Wang H, Oehlschlaeger MA, Iyer V, Iyer S, Litzinger TA, Santoro RJ, Malewicki T, Brezinsky K. "The experimental evaluation of a methodology for surrogate fuel formulation to emulate gas phase combustion kinetic phenomena." *Combust Flame*, vol. 159, no. 4, pp. 1444-1466, April 2012.

[7] Engine Combustion Network Data Archive. National Technology and Engineering Solutions of Sandia, LLC., 2017. [Online]. Available: http://www.sandia.gov/ecn/index.php. Accessed on: Sep. 29, 2017.

[8] Pickett LM, Genzale CL, Bruneaux G, Malbec LM, Hermant L, Christiansen C, Schramm J. "Comparison of diesel spray combustion in different high-temperature, high-pressure facilities." *SAE Int J Engines*, vol. 3, no. 2, pp. 156-181, Oct 2010.

[9] Pickett LM, Manin J, Genzale CL, Siebers DL, Musculus MPB, Idicheria CA. "Relationship between diesel fuel spray vapor penetration/dispersion and local fuel mixture fraction." *SAE Int J Engines*, vol. 4, no. 1, pp. 764-799, April 2011.

[10] Payri R, Garcia-Oliver JM, Bardi M, Manin J. "Fuel temperature influence on diesel sprays in inert and reacting conditions." *Appl Therm Eng*, vol. 35, pp. 185-195, March 2012.

[11] Benajes J, Payri R, Bardi M, Martí-Aldaraví P. “Experimental characterization of diesel ignition and lift-off length using a single-hole ECN injector.” *Appl Therm Eng*, vol. 58, no. 1-2, pp. 554-563, Sep 2013.

[12] Luo Z, Som S, Sarathy SM, Plmer M, Pitz WJ, Longman DE, Lu T. “Development and validation of an n-dodecaen skeletal mechanism for spray combustion applications.” *Combust Theory Model*, vol. 18, no. 2, pp. 187-203, June 2012.

[13] Pei Y, Hawkes ER, Kook S, Goldin GM, Lu T. “Modelling n-dodecane spray and combustion with the transported probability density function method.” *Combust Flame*, vol. 162, no. 5, pp. 2006-2019, May 2015.

[14] Kundu P, Pei Y, Wang M, Mandhapati R, Som S. “Evaluation of turbulence-chemistry interaction under diesel engine conditions with multi-flamelet RIF model.” *Atomization Sprays*, vol. 24, no. 9, pp. 779-800, 2014.

[15] D’Errico G, Lucchini T, Contino F, Jangi M, Bai XS. “Comparison of well-mixed and multiple representative interactive flamelet approaches for diesel spray combustion modelling.” *Combust Theory Model*, vol. 18, no. 1, pp. 65-88, Jan 2014.

[16] Bhattacharjee S, Haworth DC. “Simulations of transient n-heptane and n-dodecane spray flames under engine-relevant conditions using a transported PDF method.” *Combust Flame*, vol. 160, no. 10, pp. 2083-2102, Oct 2013.

[17] Pei Y, Hawkes ER, Bolla M, Kook S, Goldin GM, Yang Y, Pope SB, Som S. “An analysis of the structure of an n-dodecane spray flame using TPDF modelling.” *Combust Flame*, vol. 168, pp. 420-435, June 2016.

[18] Davidson DF, Haylett DR, Hanson RK. “Development of an aerosol shock tube for kinetic studies of low-vapor-pressure fuels.” *Combust Flame*, vol. 155, no. 1-2, pp. 108-117, Oct 2008.

[19] Vasu SS, Davidson DR, Hong Z, Vasudevan V, Hanson RK. “n-Dodecane oxidation at high-pressures: Measurements of ignition delay times and OH concentration time-histories.” *Proc Combust Inst*, vol. 32, no. 1, pp. 173-180, 2009.

[20] HPS Shen, Steinberg J, Vanderover J, Oehlschlaeger MA. “A shock tube study of the ignition of n-heptane, n-decane, n-dodecane, and n-tetradecane at elevated pressures.” *Energy Fuels*, vol. 23, no. 5, pp. 2482-2489, March 2009.

[21] Haylett DR, Davidson DF, Hanson RK. "Ignition delay times of low-vapor-pressure fuels measured using an aerosol shock tube." *Combust Flame,* vol. 159, no. 2, pp. 552-561, Feb 2012.

[22] Pfahl U, Fieweger K, Adomeit G. "Self-ignition of diesel-relevant hydrocarbon-air mixtures under engine conditions." *Proc Combust Inst,* vol. 26, no. 1, pp. 781-789, 1996.

[23] Zhukov VP, Sechenov VA, Starikovskii AY. "Autoignition of n-decane at high pressure." *Combust Flame,* vol. 153, no. 1-2, pp. 130-1369, April 2008.

[24] Kumar K, Mittal G, Sung CJ. "Autoignition of n-decane under elevated pressure and low-to-intermediate temperature conditions." *Combust Flame,* vol. 156, no. 6, pp. 1278-1288, June 2009.

[25] Malewicki T, Brezinsky K. "Experimental and modeling study on the pyrolysis and oxidation of n-decane and n-dodecane." *Proc Combust Inst,* vol. 34, no. 1, pp. 361-368, 2013.

[26] Ranzi E, Frassoldati A, Granata S, Faravelli T. "Wide-Range kinetic modeling study of the pyrolysis, partial oxidation, and combustion of heavy n-Alkanes." *Ind Eng Chem Res,* vol. 44, no. 14, pp. 5170-5183, Nov 2004.

[27] Biet J, Hakka MH, Warth V, Glaude PA, Battin-Leclerc F. "Experimental and modeling study of the low-temperature oxidation of large alkanes." *Energy Fuel,* vol. 22, no. 4, pp. 2258-2269, May 2008.

[28] Sarathy SM, Westbrook CK, Mehl M, Pitz WJ, Togbe C, Dagaut P, Wang H, Oehlschlaeger MA, Niemann U, Seshadri K, Veloo PS, Ji C, Egolfopoulos FN, Lu T. "Comprehensive chemical kinetic modeling of the oxidation of 2-methylalkanes from C 7 to C 20." *Combust Flame,* vol. 158, no. 12, pp. 2338-2357, Dec 2011.

[29] Mze-Ahmed A, Hadj-Ali K, Dagaut P, Dayma G. "Experimental and modeling study of the oxidation kinetics of n-undecane and n-dodecane in a jet-stirred reactor." *Energy Fuel,* vol. 26, no. 7, pp. 4253-4268, June 2012.

[30] Banerjee S, Tangko R, Sheen DA, Wang H, Bowman CT. "An experimental and kinetic modeling study of n-dodecane pyrolysis and oxidation." *Combust Flame,* vol. 163, pp. 12-30, Jan 2016.

[31] Cai L, Pitsch H, Mohamed SY, Raman V, Bugler J, Curran H, Sarathy SM. "Optimized reaction mechanism rate rules for ignition of normal alkanes." *Combust Flame,* vol. 173, pp. 468-482, Nov 2016.

[32] Narayanaswamy K, Pepiot P, Pitsch H. "A chemical mechanism for low to high temperature oxidation of n-dodecane as a component of transportation fuel surrogates." *Combust Flame,* vol. 161, no. 4, pp. 866-884, April 2014.

[33] Wang H, Ra Y, Jia M, Reitz RD. “Development of a reduced n-dodecane-PAH mechanism. and its application for n-dodecane soot predictions.” *Fuel*, vol. 136, pp. 25-36, Nov 2014.

[34] Frassoldati A, D’Errico G. Lucchini T. Stagni A, Cuoci A, Faravelli T, Onorati A, Ranzi E. “Reduced kinetic mechanisms of diesel fuel surrogate for engine CFD simulations.” *Combust Flame,* vol. 162, no. 10, pp. 3991-4007, Oct 2015.

[35] Shen HPS, Oehlschlaeger MA. “The autoignition of C8H10 aromatics at moderate temperatures and elevated pressures.” *Combust Flame,* vol. 156, no. 5, pp. 1053-1062, May 2009.

[36] Wang W, Gowdagiri S, Oehlschlaeger MA. “The high-temperature autoignition of biodiesels and biodiesel components.” *Combust Flame,* vol. 161, no. 12, pp. 3014-3021, Dec 2014.

[37] Ra Y, Reitz RD. “A combustion model for multi-component fuels using a physical surrogate group chemistry representation (PSGCR).” *Combust Flame,* vol. 162, no. 10, pp. 3456-3481, Oct 2015.

[38] Cai L, Pitsch H. “Mechanism optimization based on reaction rate fuels.” *Combust Flame*, vol. 161, no. 2, pp. 405-415, Feb 2014.

[39] Sheen DA, Wang H. “The method of uncertainty quantification and minimization using polynomial chaos expansions.” *Combust Flame,* vol. 158, no. 12, pp. 2358-2374, Dec 2011.

[40] Ciezki HK, Adomeit G. “Shock-tube investigation of self-ignition of n-heptane-air mixtures under engine relevant conditions.” *Combust Flame,* vol. 93, no. 4, pp. 421-433, June 1993.

[41] Fieweger K, Blumenthal R, Adomeit G. “Self-ignition of S.I. engine model fuels: A shock tube investigation at high pressure.” *Combust Flame,* vol. 109, no. 4, pp. 599-519, June 1997.

APPENDIX

Appendix A: Ignition delay measurements for ϕ = 1.0 n-dodecane/air.

Table A.1 Ignition delay measurements for ϕ = 1.0 n-dodecane/air.

P [atm]	T [K]	τ [ms]	P [atm]	T [K]	τ [ms]	P [atm]	T [K]	τ [ms]
44.5	774	417	61.6	830	209	77.4	801	195
43.3	790	407	63.2	865	169	84.2	850	144
44.2	815	273	60	902	188	74.4	864	127
42.5	831	257	63.1	930	190	79.6	883	148
43.5	877	242	62.3	936	228	76.4	896	137
38.9	886	310	55.3	979	247	85.3	932	160
42.9	914	316	56.8	1001	215	81	966	150
39.8	954	303	60.1	1033	149	77.7	1027	141
39.3	987	332	57.9	1072	120	82.3	1064	97
41.5	1025	260	64.9	1091	105			
38.4	1050	192	61.9	1124	70			
39.6	1065	179						
36.6	1132	108						
38.1	1163	65						

Table A.2 Ignition delay measurements for ϕ = 2.0 n-dodecane/air.

P [atm]	T [K]	τ [ms]	P [atm]	T [K]	τ [ms]
39.2	802	256	63.1	821	202
39	803	253	62	854	147
38.5	813	230	61	891	154
41.6	838	209	60.1	929	155
43.4	848	191	61.5	970	178
42.4	927	234	58.5	986	172
38	934	250	57.7	1040	121
40.9	999	246	58.2	1089	78
36.4	1030	185	60.1	1104	75
37	1088	128			
38.7	1121	82			

Table A.3 Ignition delay measurements for ϕ = 1.0 n-dodecane/15% O_2/N_2.

P [atm]	T [K]	τ [ms]
64.2	840	347
62	879	297
63.1	904	299
64.7	947	344
60.2	989	373
59.2	1012	275
61.5	1062	188
58.1	1078	141
57.7	1112	114

Table A.4 Ignition delay measurements for ϕ = 1.0 n-dodecane/13% O_2/N_2.

P [atm]	T [K]	τ [ms]
65.3	841	434
64.1	873	354
62.7	928	416
63	948	453
61.3	978	446
60.2	1013	352
61.5	1057	229
59.6	1081	181
58	1112	140
58.7	1139	91